The Theory of Scintillation Revisited

Charles L. Rino

May 22, 2025

Abstract

"The Theory of Scintillation *with* Applications in Remote Sensing" was published in 2011. The website https://chuckrino.com was started as a forum for discussing remote sensing applications of electromagnetic (EM) wave propagation in transparent media. The underlying phenomenon is electromagnetic (EM) wave propagation in transparent media, specifically the earth's ionosphere and atmosphere. EM waves are vector fields governed by Maxwell's equations. Linear constitutive relations characterize the EM field interactions with propagation media. Scintillation refers to irregular variations imparted to signal parameters that have traversed structured regions.

The physical processes that cause structure development comprise an engaging theory in its own right. Propagation theory connects parameterized remote diagnostic observables with complementary parameterized measures of the in situ structure. Parameters can be estimated with established procedures that reconcile diagnostic measurements with the theoretical predictions.

In the decade that has passed since the book was published more refined interpretations have revealed limitations and new applications of the theory. A set of MatLab procedures accompanied the publication. This report is the first part of a review and update of the original publication and MatLab procedures.

1 Introduction

Formally, scintillation is a stochastic modulation imparted to electromagnetic (EM) fields propagating in transparent inhomogeneous media. EM fields initiated by the sun and a plethora of other extraterrestrial sources provided the earliest scintillation observations. Following the launch of Sputnik in 1957 [REF] artificial earth satellite sources began to supplement natural sources. The Wideband Satellite, launched in 1976, was dedicated to scintillation observations. The first global positioning satellites (GPS) were launched in 1978 [REF]. When "The Theory of Scintillation *with* Applications in Remote Sensing" Rino [1] (hereafter *ScintTheory*) was published in 2011, the global navigation satellite system (GNSS) was becoming the primary source of ionospheric

structure diagnostics. This document reviews *ScintTheory* in light of new theoretical insights and new diagnostic applications.

Propagation theory provides the theoretical framework for characterizing the structure imparted to EM fields propagating in structured media. With a formal incorporation of stochastic processes statistical measures of the evolving fields can be related analytically to statistical measures of the media structure. For real-world applications the transition between structure that admits analytic characterization and structure that can be characterized only with statistical measures must be identified. The desired end result is a complementary set of simulation and diagnostic procedures supported by a common theory.

The statistical theory summarized in Chapter 3 of *ScintTheory* is confined to propagating fields that subtend a narrow range of propagation angles. The development follows from a *forward propagation equation* (FPE), which is a generalization of widely used multiple phase screen (MPS) split-step integration. The generalization replaces the parabolic propagator normally used for MPS applications with a an exact wide-angle propagator. Recent applications of the FPE to HF propagation was demonstrated in two Rino and Carrano companion papers [2] and [3]. A disparity was found between FPE calculations of a narrow HF beam refracted by an ionospheric layer and ray-trace calculations of the beam trajectory. The source of the disparity was an inconsistent application of the unrestricted propagation operator. This document revisits the development in the Rino and Carrano papers to identify FPE limitations and introduce alternative albeit computationally demanding procedures that are well know in acoustic and seismic applications of propagation theory. Whereas theoretical results derived from the restricted FPE fully accommodate GNSS diagnostic measurements, the extension to HF remains a work in progress that will be summarized.

2 Propagation in Inhomogeneous Media

Chapters 1 and 2 of *ScintTheory* developed a first-order differential equation [1], which was referred to as the forward propagation equation (FPE). The multiple phase screen (MPS) method is formally a split-step integration of the FPE. All subsequent results in *ScintTheory* followed from the FPE. The theoretical results that comprise the statistical theory of scintillation, as summarized in Chapter 3 of *ScintTheory*, are applicable only to fields that subtend a narrow range of propagation angles, whereas the MPS propagator is unrestricted. This seems to imply that the FPE is more general than the parabolic wave equation. However, applications of the FPE at HF frequencies revealed a disparity between refracted narrow beam fields and ray theory predictions. The source of the disparity was known in scalar acoustic propagation theory. Here we review the development in Rino and Carrano [2] to provide a consistent treatment of forward propagation in inhomogeneous media with large-scale and small-scale structure.

[1] Equation (2.2) in *ScintTheory*.

The starting point is Maxwell's equations. We assume that the media structure evolves slowly enough to be *frozen* over typical measurement intervals. Under this assumption Maxwells equations can be written in the following time-harmonic form with no further limiting assumptions:

$$\nabla \times \mathbf{E} = -i\omega\mathbf{B} \tag{1}$$

$$\nabla \times \mathbf{H} = i\omega\mathbf{D} \tag{2}$$

$$\mathbf{B}{=}\mu_0\mathbf{H} \tag{3}$$

$$\mathbf{D} = \epsilon_0\overline{\epsilon} \cdot \mathbf{E} = 0, \tag{4}$$

The vector fields $\mathbf{E}$ and $\mathbf{H}$ represent electric and magnetic field intensities. The vector fields $\mathbf{D}$ and $\mathbf{B}$ represent electric and and magnetic induction fields. The temporal $f = \omega/(2\pi)$ frequency in Hz with ω is the radian angular frequency. The parameters μ_0 and ϵ_0 are fundamental constants that define the speed of light,

$$c = 1/\sqrt{\mu_0\epsilon_0}. \tag{5}$$

The dielectric tensor, $\overline{\epsilon}$, is defined as

$$\overline{\epsilon} = \overline{I} + X\overline{\chi}, \tag{6}$$

where $\overline{I}$ is the identity matrix and $X\overline{\chi}$ is the susceptibility matrix, which is written as a product of a spatially varying scalar and a 3×3 tensor. Departures from homogeneity are defined by the frequency-dependent scalar, X. A complete definition of $X\overline{\chi}$ for the standard ionosphere is presented in the Rino and Carrano [2] appendix, which includes the Appleton Hartree equations. All the quantities have time implicit time variation $\exp\{i\omega t\}$. The formulation characterizes the spatial evolution of fields initiated by an impressed source field.

From (1) and (3) with substitutions from (2) and (4) a single vector equation for $\mathbf{E}$ can be derived. The vector wave equation follows after substitution of a standard vector identity for $\nabla \times \nabla \times \mathbf{E}$:

$$\nabla^2\mathbf{E}(\mathbf{r}) + k^2\mathbf{E}(\mathbf{r}) = -X(\mathbf{r})\overline{\chi}\mathbf{E}(\mathbf{r}) + \nabla\left(\nabla \cdot \mathbf{E}\right) \tag{7}$$

Regarding the divergence , $\nabla \cdot \mathbf{E}$, the textbook "Waves and Fields in Inhomogeneous Media" Chew [4] avoids explicit treatment of the divergence term by accommodating only homogeneous subregions defined by discontinuous boundaries, e. g. layers and discrete scatterers. Within homogeneous subregions $\nabla \cdot \mathbf{E} = 0$**.** Induced sources on the boundaries support discontinuous field changes. Strictly speaking, only a homogeneous medium can support divergence-free $\mathbf{E}$ and $\mathbf{H}$ fields. For example if we let

$$\overline{\chi} = \mathbf{V}^{-1}\overline{D}\mathbf{V}, \tag{8}$$

where $\overline{D}$ is a diagonal matrix of eigen values and the columns of $\mathbf{V}$ are eigen vectors, substituting $\mathbf{V}^{-1}\mathbf{E}(x,\rho)$ into the wave equation with $\nabla \cdot \mathbf{E} = 0$ leads

to independent scalar wave equations, which cannot change the direction of the vector fields. Consequently, solutions to the scalar wave equation

$$\nabla^2\psi(\mathbf{r}) + k^2\psi(\mathbf{r}) = -X(\mathbf{r})\overline{\chi}\psi(\mathbf{r}), \tag{9}$$

which conserve total intensity, must be interpreted as projections of the vector field.

To facilitate numerical exploration, structure variation will be confined to the xy plane, with no variation along the z axis. Two-dimensional propagation theory is characterized by the scalar wave equation

$$\nabla^2\psi\left(x,y\right) + k^2\psi\left(x,y\right) = -k^2X\left(x,y\right)\psi\left(x,y\right). \tag{10}$$

For ionospheric profiles

$$X\left(x,y\right) = 4\pi N_e\left(x,y\right)/(r_e k^2) \tag{11}$$

where N_e is the electron density and $r_e = 2.819740289 \times 10^{-15}$ m is the classical electron radius. Directed propagation will be defined with respect to the x axis. Consider an initiating field

$$\psi_0(y) = \int \widehat{\psi}_0(\kappa)\exp\{-i\kappa y\}\frac{d\kappa}{2\pi}. \tag{12}$$

Substitution into (10) will show that

$$\psi(x,y) = \int \widehat{\psi}_0(\kappa)\exp\{\pm ik\sqrt{1-(\kappa/k)^2}x\}\exp\{i\kappa y\}\frac{d\kappa}{2\pi} \tag{13}$$

$$= \int \widehat{\psi}_0(\kappa)\exp\{\pm ik\sqrt{1-(\kappa/k)^2}x + \kappa y\}\frac{d\kappa}{2\pi} \tag{14}$$

satisfies the homogeneous equation. The second form emphases the interpretation of freely propagation fields as independently propagating plane waves defined by the wave vector

$$\mathbf{k} = [\pm k_x(\kappa), \kappa] \tag{15}$$

$$k_x(\kappa) = k\sqrt{1-(\kappa/k)^2} \tag{16}$$

At this point κ is unresticted, although the sign of $k_x(\kappa)$ must be chose so that evanescent contributions from $|\kappa| < k$ are damped.

2.1 Induced Source Methods

Using the formal Green's function property

$$\nabla^2 H(x,y) + k^2 H(x,y) = -\delta(x-x', y-y'), \tag{17}$$

solutions to the scalar wave equation satisfy the integral equation for

$$\psi(x,y) = \psi_0(x,y) - k^2 \iint \psi(x',y')X(x',y') \times H(x-x',y-y')dx'dy', \tag{18}$$

which includes the source field, $\psi_0(x,y)$, explicitly. The structure contribution is effectively an induced source. The induced source form shows that every point in the propagation space potentially affects every other point. Solving the integral equations amounts to reconciling all the interactions.

The Fourier transformation

$$\int H_0^{(1)}(k\rho)/(4i)\exp\{-ik\kappa y\}dy = \frac{1}{2i}\frac{\exp\{ikg(\kappa)\,|x|\}}{kg(\kappa)}\exp\{ik\kappa y\}, \tag{19}$$

follows from the Weyl representation

$$\int H_0^{(1)}(k\rho)/(4i)\exp\{-ik\kappa y\}dy = \frac{1}{2i}\frac{\exp\{ikg(\kappa)\,|x|\}}{kg(\kappa)}\exp\{ik\kappa y\}. \tag{20}$$

Using (20), (18) can be transformed to the spatial Fourier domain

$$\widehat{\psi}(\kappa;x) = \widehat{\psi}_0(\kappa;x) - k^2\int_0^\infty \int \psi(x',y')X(x',y')\exp\{-ik\kappa y'\}dy' \times \frac{1}{2i}\frac{\exp\{ikg(\kappa)|x-x'|\}}{kg(\kappa)}dx'. \tag{21}$$

At this point the summation of waves propagating in the positive (forward) and negative (backward) x directions must be treated explicitly. Two coupled forward and backward equations can be derived. The forward approximation neglects backward propagating waves initiated where $x' > x$:

$$\widehat{\psi}^+(\kappa;x) = \widehat{\psi}_0(\kappa;x) - k^2\int_0^x \int \psi^+(x',y')X(x',y')\exp\{-ik\kappa y'\}dy' \times \frac{1}{2i}\frac{\exp\{ikg(\kappa)(x-x')\}}{kg(\kappa)}dx'. \tag{22}$$

For a small forward increments

$$\widehat{\psi}(\kappa;x+\Delta x) = \widehat{\psi}(\kappa;x)\exp\{ikg(\kappa)\Delta x\}+ \frac{ik}{2g(\kappa)}\int_0^{\Delta x}\left[\int \psi(x+x',y')X(x+x',y') \times \int \psi(x+x',y')X(x+x',y')\right]dx'. \tag{23}$$

The derivation here follows the development in Rino and Carrano [2]. The problem is no fully consistent evaluation of the term in square brackets will preserve the implied additive separation of propagation and media-interaction terms. As Louis Fishman has put it, the differential equations:

$$\frac{\partial\widehat{\psi}(\kappa;x)}{\partial x} = ikg(\kappa)\left[\psi(\kappa;x) + 1/\left(2g(\kappa)^2\right)\int \psi(x,y') \times X(x,y')\exp\{-ik\kappa y'\}dy'\right] \tag{24}$$

$$\frac{\partial\psi(x,y)}{\partial x} = \Theta\psi(x,y) + k^2\int H_0^{(1)}(k\,|y'-y|)/\,(4i)\,\psi(x,y')X(x,y')dy' \tag{25}$$

where $\Theta\psi(x,y)$ represents an incremental free propagation step, are just plain wrong! . At best, the FPE defined as

$$\frac{\partial\psi(x,y)}{\partial x} = \Theta\psi(x,y) - i\frac{k}{2}X(x,y)\psi(x,y). \tag{26}$$

can be applied reliably only when the parabolic form of the propagation operator is used. Bremmer series applications [5], have yet to produce tractable induced-source methods. Effectively, induced source methods are restricted to fields that subtend a narrow range of propagation angles.

2.2 Factorization Methods

An alternative approach to constructing solutions to (10) uses a formal factorization. Rewriting the Laplacian as a differential operator,

$$\nabla^2 = \partial^2/\partial x^2 + \nabla_\perp^2, \tag{27}$$

identifies the x axis as a propagation reference. The differential operator form of the wave equation,

$$\left(\frac{\partial^2}{\partial x^2} + \nabla_\perp^2 + k^2K(x,y)^2\right)\psi(x,y) = 0, \tag{28}$$

where

$$K(x,y)^2 = I + X(x,y), \tag{29}$$

can be formally factored to as

$$\begin{aligned}&\frac{\partial^2}{\partial x^2} + \nabla_\perp^2 + k^2K(x,y)^2\\ &= \left(\frac{\partial}{\partial x} - i\left(\nabla_\perp + k^2K(x,y)^2\right)^{1/2}\right)\\ &\times\left(\frac{\partial}{\partial x} + i\left(\nabla_\perp + k^2K(x,y)^2\right)^{1/2}\right).\end{aligned} \tag{30}$$

The factorization is strictly valid only if the factored components commute, which would eliminate variation along the propagation direction. However, commutation equivalence is necessary only over are integration steps.

The operator factorization form of the forward propagation equation is

$$\left(\frac{\partial}{\partial x} - i\left(\nabla_\perp + k^2 K(x,y)\right)^{1/2}\right)\psi(x,y) = 0. \tag{31}$$

Approximating the square root operator with the first term ina Taylor series expansion leads to the parabolic wave equation or Feit-Fleck approximation [6], which is equivalent to the FPE with the propagation operator replaced by its parabolic form. A formal operator extension to propagation in inhomogeneous media has the general form

$$\psi(x,y) = \int \widehat{\psi}(x;\kappa)\exp\{i\Omega(x;\kappa,K(x,y))\}\exp\{-i\kappa(y-y')\}\frac{d\kappa}{2\pi}, \tag{32}$$

where $\Omega(x,y;\kappa,K(x,y))$ is the spectral-domain counterpart of the square-root operator developed in a series of papers by Fishman [7] [8] [9]. An intuitively appling approximation

$$\Omega(x;\kappa,K(x,y)) = \sqrt{K(x,y)^2 - (\kappa/k)^2}x, \tag{33}$$

can be applied over incremental slabs. The approximation was rediscovered in acoustics by [10]. However, the y variation precludes efficient FFT evaluation, which makes evaluation very time consuming.

2.3 Parabolic Differential Equation Methods

The square root operator can be approximated by implementing analytic approximations to the square-root function. The approximation is improved by substituting $\psi(x,y) = \exp\{ikx\}U(x,y)$ in the operator form of the wave equation:

$$\left(\frac{1}{k^2}\frac{\partial^2}{\partial x^2} - 1 + K(x,y)^2 + \nabla_\perp^2/k^2\right)U(x,y) = 0. \tag{34}$$

Following Collins, [11], the PDE can written as

$$\frac{\partial U(x,y)}{\partial x} = ik\left(-1 + \sqrt{1+X_P}\right)U(x,y) \tag{35}$$

where

$$X_P = K(x,y)^2 + \nabla_\perp^2/k^2. \tag{36}$$

The Pade approximation, which treats X_P as a complex variable, is defined in terms of precalculated coefficients such that

$$-1 + \sqrt{1+X_P} \simeq \sum_{j=1}^{n}\frac{\alpha_{j,n}X_P}{1+\beta_{j,n}X_P}. \tag{37}$$

A split-step solution is implemented with phase corrections,

$$u(x+\Delta x) = \exp\{ik\Delta x(-1+\sqrt{1+X_P})\}u(x), \tag{38}$$

which leads to the replacement of the summation by a product form

$$\prod_{j=1}^{n} \frac{1+\lambda_{j,n}X_P}{1+\mu_{j,n}X_P}. \tag{39}$$

Recognizing that X_P contains second derivatives, the coefficients are chosen to ensure that the differential-equation solution is stable and accurate. The PDE method has produced accurate forward propagation solutions. However, selections of coefficients and sampling is problem specific.

The book "Parabolic equation methods for electromagnetic wave propagation," by Levy [12] presents a complete treatment of parabolic wave equation (PWE) methods including stochastic structure, and boundaries.

2.4 Eigenvector Methods

As demonstrated in Collins and Segman [11], the most demanding inhomogeneous media problems can be implemented with the Pade approximation. However, there is a way to construct an exact solution to the forward approximation

$$\frac{\partial\psi(x,y)}{\partial x} = ikQ(x,y)\psi(x,y),$$

where

$$Q = k\sqrt{1+X+\nabla_\perp^2/k^2}. \tag{40}$$

Following [13], consider the formal vector matrix solution

$$\overrightarrow{\psi} = \exp\{ik\Delta x\overleftrightarrow{Q}\}\overrightarrow{\psi} \tag{41}$$

where $\overleftrightarrow{Q}$ is a matrix square root. To interpret the matrix operator $\overleftrightarrow{Q}$, let

$$\rho_n = \exp\{2\pi in/N\}, \tag{42}$$

which is an eigenvector or the matrix form of the discrete Fourier transform (DFT):

$$\begin{array}{l}\overleftrightarrow{R} = [\rho_n^m] \; n => \text{ col}, \; m => \text{row} \\ \overleftrightarrow{R}\overrightarrow{\psi},\end{array} \tag{43}$$

where $\overleftrightarrow{R}'\overleftrightarrow{R}$ =diag$(1/N)$. It follows that with

$$\overleftrightarrow{K} = -\text{diag}(\,(\kappa_n/k)^2\,) \tag{44}$$

The matrix argument of the square root can be written as

$$\overleftrightarrow{Q} = \sqrt{\overleftrightarrow{R}'\overleftrightarrow{K}\overleftrightarrow{R}/N + \mathrm{diag}(1 + X_y)} \tag{45}$$

There is an exact solution for $X_y = 0$. Rewriting $\overleftrightarrow{Q}$ as

$$\overleftrightarrow{Q} = \sqrt{\overleftrightarrow{R}'(\overleftrightarrow{K} + \overleftrightarrow{I})\overleftrightarrow{R}/N} \tag{46}$$

the eigen vectors of

$$\overleftrightarrow{Q}^2 = \overleftrightarrow{R}'(\overleftrightarrow{K} + \overleftrightarrow{I})\overleftrightarrow{R}/N \tag{47}$$

are the column vectors of $\overleftrightarrow{R}/\sqrt{N}$ A formal matrix solution that advances any starting field can be constructed as follows

$$\overrightarrow{\psi} = \overleftrightarrow{R}\left(\left(\overleftrightarrow{R}'\overrightarrow{\psi}_0\right)\exp\left\{-k\Delta x\sqrt{\mathrm{diag}(1-(\kappa_n/k)^2)}\right\}\right); \tag{48}$$

which can be rewritten as

$$\overrightarrow{\psi} = \left(\overleftrightarrow{R}'\overrightarrow{\psi}_0\right)\exp\left\{-k\Delta x\sqrt{\mathrm{diag}(1-(\kappa_n/k)^2}\right\}\overleftrightarrow{R} \tag{49}$$

The computation follows from an eigenvector decomposition of $\overleftrightarrow{Q}^2$

$$\overleftrightarrow{Q}^2 = \overleftrightarrow{\Xi}'\overleftrightarrow{\Lambda}\overleftrightarrow{\Xi}. \tag{50}$$

The same eigenvectors define $\overleftrightarrow{Q}$

$$\overleftrightarrow{Q} = \overleftrightarrow{\Xi}'\sqrt{\overleftrightarrow{\Lambda}}\overleftrightarrow{\Xi}' \tag{51}$$

The final solution is

$$\overrightarrow{\psi} = \overleftrightarrow{\Xi}'\exp\{ik\Delta x\sqrt{\overleftrightarrow{\Lambda}}\}\overleftrightarrow{\Xi}\overrightarrow{\psi_0} \tag{52}$$

As a consistency check for free space

$$diag(\overleftrightarrow{\Lambda}) = \sqrt{1-(\kappa_n/k)^2}),\ \overleftrightarrow{\Xi} = R/\sqrt{N}. \tag{53}$$

In effect, the complexity of implementing the Pade approximation has been traded for the complexity of computing the eigenvectors of a large matrix. However, robust eigenvector utilities are available. For exploration purposes, the ease of implementation make eigenvector solutions very attractive.

2.5 Ray Optics

Whether FPE, PDE, or OHE solutions are implemented, other than internal consistency it is desirable to have a exact result for verification. With $\overline{\chi} = I$, the formally exact defining equation is

$$\nabla^2\mathbf{E}+k^2\mathbf{E} = \nabla(\nabla\cdot\mathbf{E}) - k^2X\mathbf{E}. \tag{54}$$

Ray optics is based on the assumption that the field associated with a propagating field can be apporoximated locally as single plane wave with a slowly vary amplitude and a smoothly varying phase. Following the development in Born and Wolf [14, Chapter 3.2], $\mathbf{E}(\mathbf{r})$ is approximated as

$$\mathbf{E}(\mathbf{r}) = \widetilde{\mathbf{E}}(\mathbf{r})\exp\{ik\vartheta(\mathbf{r})\}. \tag{55}$$

Inserting (55) into the vector wave equation and retaining only terms that are first-order in ΔX leads to the to the defining equation

$$(\nabla\vartheta)^2 = n^2, \tag{56}$$

where

$$n^2 = 1 + X. \tag{57}$$

The identification of n as a refractive index follows from the definition

$$\nabla\vartheta = \mathbf{n} \tag{58}$$

where $\vartheta = k\mathbf{n}\cdot\mathbf{r}$. Wavefronts are defined by contours of constant ϑ. If s represents distance along a *ray*, normal to $\nabla\vartheta$, the defining equation can be rewritten as

$$n\frac{d\mathbf{r}}{ds} = \nabla\vartheta. \tag{59}$$

Eliminating ϑ, leads to the ray equation

$$\begin{aligned}\frac{d}{ds}\left(n\frac{d\mathbf{r}}{ds}\right) &= \nabla n\\ \frac{d^2\mathbf{r}}{ds^2} + \frac{dn}{nds}\frac{d\mathbf{r}}{ds} &= \frac{\nabla n}{n}.\end{aligned} \tag{60}$$

Let

$$\tau = \frac{d\mathbf{r}}{ds}, \tag{61}$$

whereby

$$\frac{d\tau}{ds} + \frac{dn}{nds}\tau = \frac{\nabla n}{n} \tag{62}$$

$$\frac{d\tau}{ds} + \mathbf{s}\cdot\left(\frac{\nabla n}{n}\right)\tau = \left(\frac{\nabla n}{n}\right), \tag{63}$$

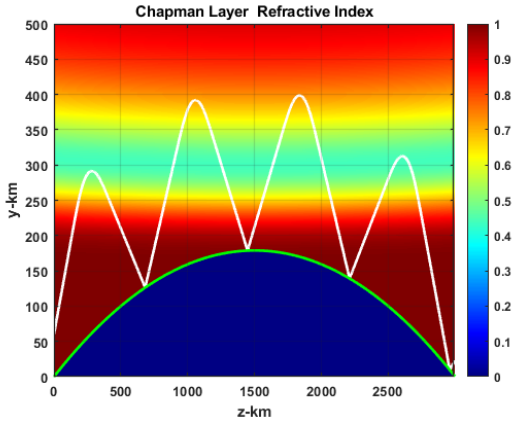

Figure 1: Chapman layer over curved earth with ray trace overlaid.

where **s** is a unit vector along the ray direction. The defining ray equations are fully three dimensional an impose no constraint on the structure other than a self checking smoothness. Reflecting boundaries are readily accommodated.

A complete treatment of ray theory and its extension to vector fields is demanding and leads to advanced mathematical procedures. For example, the ray theory in the seminal text "The propagation of radio waves," by Budden [15] is not presented until Chapter 14. The implementation of the Haselgrove equations requires variational calculus methods Colman [16]. However, for our purposes here an implementation of the ray equations here will suffice.

3 Examples

3.1 Ray Trace

A two-dimensional propagation calculation is defined by a height, a propagation distance, a starting field, a specification of X and frequency, f. An absorbing upper boundary accommodates escaping energy. A reflecting surface or implementation of the forward boundary method described in Rino and Carrano [3] reflects fields at the lower boundary. Current implementations of the PDE and OHE solutions accommodate conducting boundary surfaces with Dirichlet boundary conditions. Figure 1 shows a Chapman layer at 300 km over a smooth spherical-earth boundary. A ray trace from the source at 50 kM is overlaid. A direct implementation of (60) modified to reflect rays from a smoothly varying boundary surface was used to calculate ray paths. For this application, y represents height and z represents propagation distance. There is no variation along x. Altitude is measured along normal radials from the surface as a function of y and z. A layer at a fixed distance from a curved surface creates a range-dependent propagation environment.

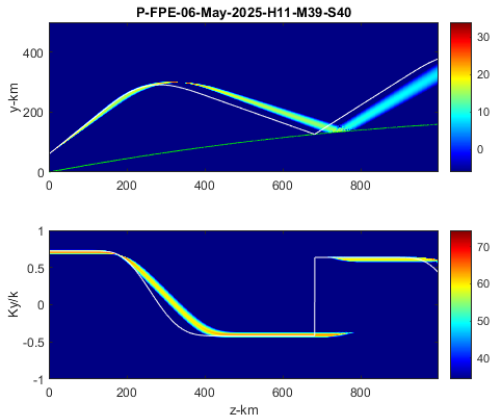

Figure 2: Upper frame FPE intensity with ray path overlay.

3.2 FPE

Although the complete propagation grid was used for the FPE simulations in Rino and Carrano [2], [3], SSPDE and OHE applications require significantly more computation.

A smaller truncated propagation space is used. The upper frame of Figure 2 shows the FPE field intensity for beam propagation into a refracting Chapman layer. A ray trace initiated at the 20 km source height with the measured beam direction is overlaid (white). The lower frame shows the spectral intensity with the ray trace direction overlaid. As consistently observed with FPE propagation in highly refractive environments, the FPE solution under estimates refraction. However, without the ray trace for comparison the error might not be noticed. The upper frame in Figure (3) shows the total intensity of the FPE field, which is invariant as long as the field is confined to the propagation space. The loss at the surface reflection is caused by the shift-map implementation of the boundary variation. The lower frame shows the spectral domain peak intensity with the ray direction overlaid, which varies in response to induced waveform variations.

3.3 SSPDE

Figures 4 and 5 summarize an SSPD simulation of the Chapman layer environment with a plane conducting layer. The upper frame in 4 summarizes the beam intensity with the ray trace overlaid. The lower frame shows the spectral intensity with the ray direction overlaid. The spectral domain peak does not align with the ray direction evidently because of the distortion of the spectrum as the beam peak narrows in response to the interaction with layer. Figure 5 shows the integrated intensity and the beam peak intensity, which increases and decreases in response to induced beamwidth changes. The vertical sampling is

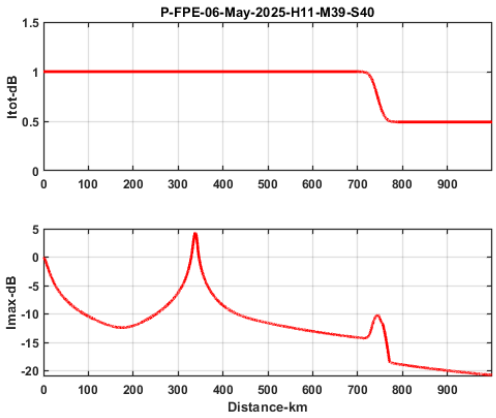

Figure 3: Upper frame shows the integrated intensity of the field, which should be 1. The lower frame shows the spectral domain peak intensity.

12 per wavelength, 6 samples per wavelength along the propagation direction, and 8 Pade coefficients. The over sampling and the number of Pade coefficients was determined by trial and error.

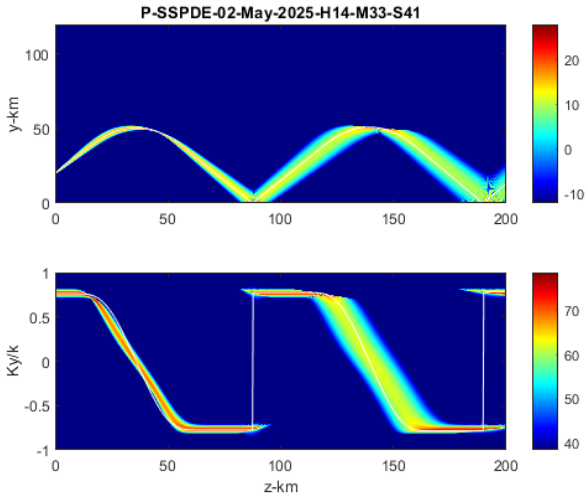

Figure 4: SSPD intensity (upper frame) and spectral intensity (lower frame).

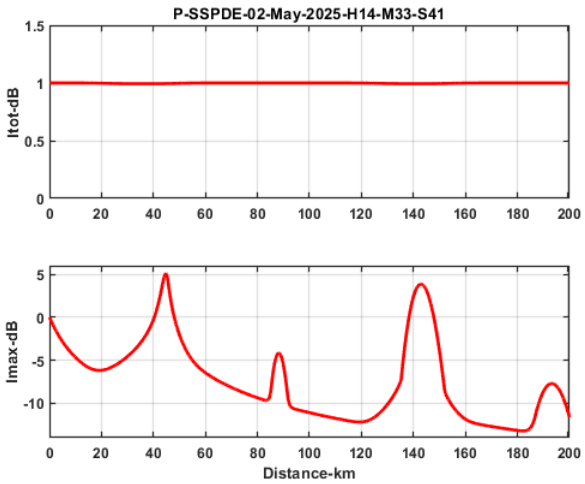

Figure 5: SSPDE total intensity (upper frame) and peak intensity (lower frame).

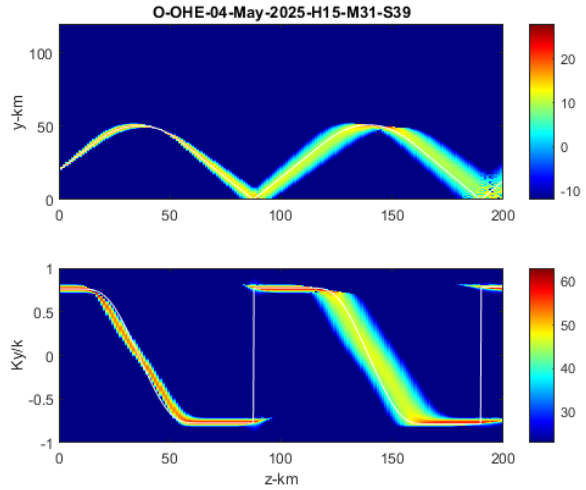

Figure 6: OHE intensity (upper frame) and spectral intensity (lower frame).

3.4 OHE

Figures 6 and 7 summarize the OHE calculation. The OHE calculation is performed with the same critical sampling used for the FPE calculation. The eigenvector computation is computationally demanding. However, for propagation in a transversely inhomogeneous medium only one evaluation is needed. It is encouraging that results from two dissimilar methods give nearly identical results.

Belyaev et. al [13] computed the refraction of a beam injected into a neutral layer, which effectively trapped the beam. Figure 8 shows a similar calculation at 10 MHz. The overlaid ray trace required height and direction adjustments to achieve agreement with the wave intensity peak. The ray angle is consistently calculated, but shows significant departures from the wave spectrum peak. Figure 9 shows the waveform intensity and spectrum at the point of maximum departure of the ray angle from the spectral domain peak. Because of the asymmetry the spectral peak is displaced from the true waveform direction.

3.5 Commutation limitation

Factorization methods are strictly valid only if there is no range variation. However, if range variation is neglibible over a propagation step, SSPDE and OHE is constrained mainly by sampling. Although the propagation environment defined by a layer above a curved surface is range dependent, a more stringent variation is realized by a lens like symmetric gaussian structure. Figure 10 shows the gaussian lens refractive index with horizontally initiated rays over-

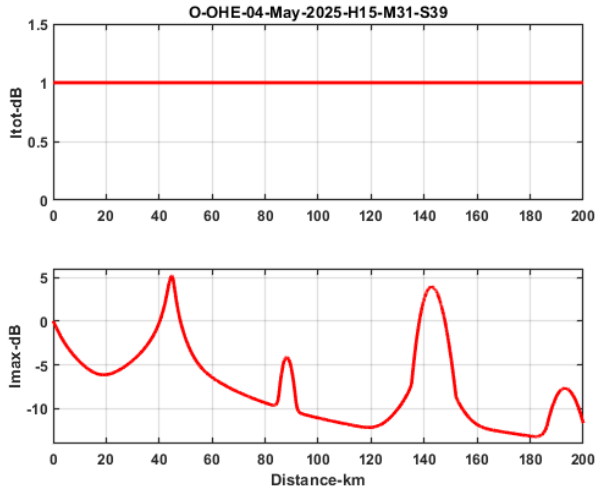

Figure 7: OHE total intensity (upper frame) and peak intensity (lower frame).

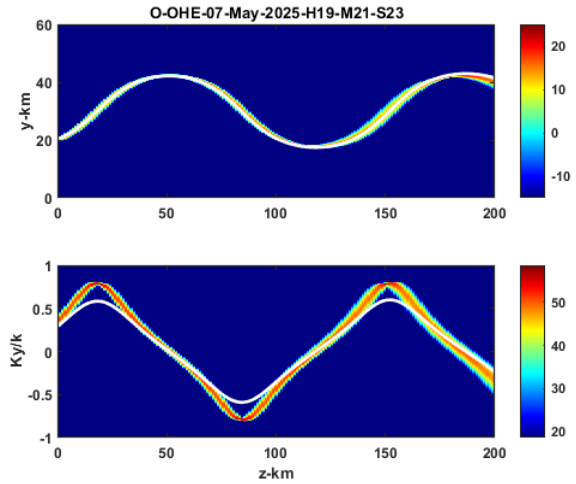

Figure 8: OHE example of refraction by a gaussian layer.

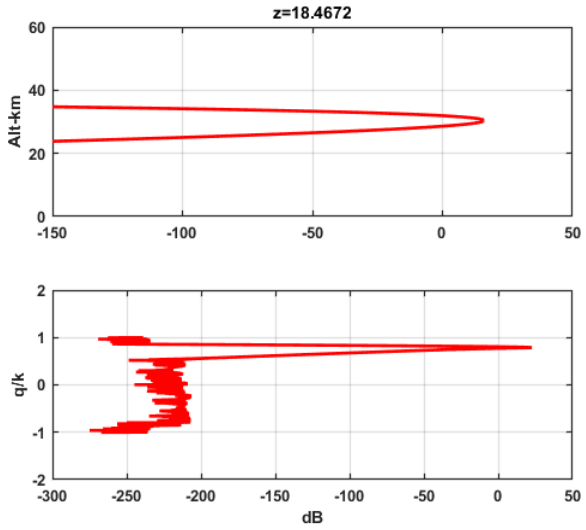

Figure 9: OHE waveform and spectrum at the point of maximum ray direction separation.

laid. A well designed lens will refract incident parallel rays to a focal point as shown. For verifying SSPDE two-horizontal beams were symetrically located about the beam center. Figures 11 and 12 summarize the result. The SSPDE captures the focal point defined by the intersection of the beam rays accurately, which indicates the smooth range do not translate to comutation errors.

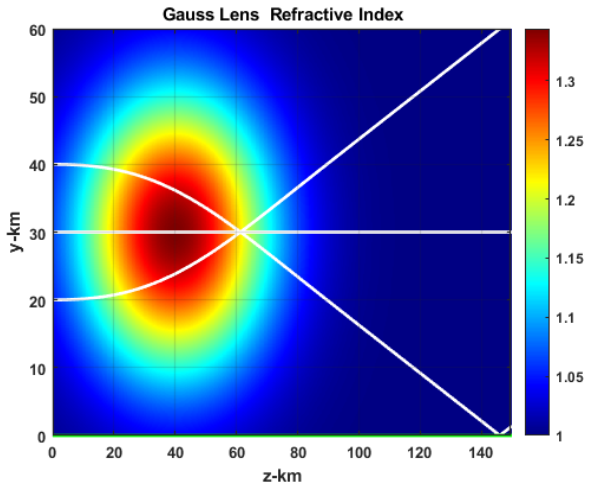

Figure 10: Refractive index of gaussian lens with horizontially initiated rays overlaid.

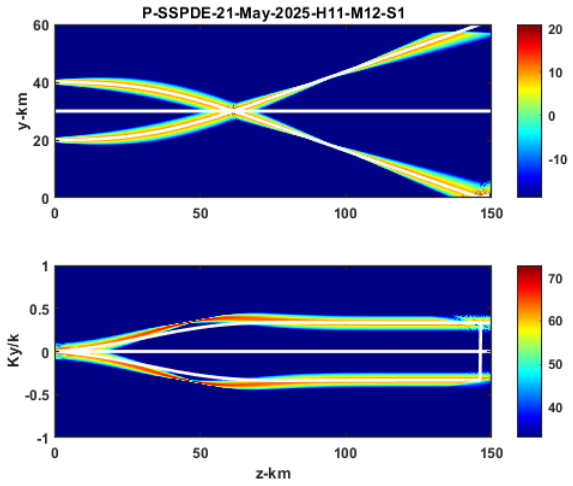

Figure 11: Summary of SSPDE parallel beam propagation through gaussian lense with ray traces overlaid.

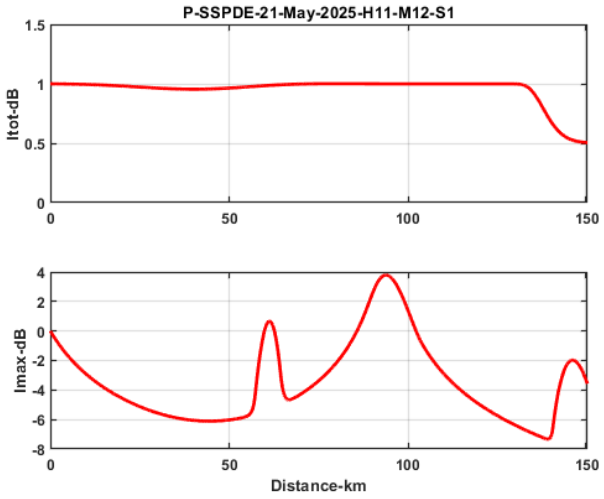

Figure 12: Total intensity (upper frame) and peak intensity (lower frame) of SSPDE simulation of parallel beam field.

4 Summary of Propagation in Smoothly Varying Media

Developing tractable methods for calculating propagation in smoothly varying media remains a work in progress as well as validating procedures for incorporating structure. The problem becomes acute when it is necessary to identify characteristic with accurate polarization predictions. The scalar codes demonstrated provide starting points and guidelines. Results should be viewed guardedly.

References

[1] Charles L. Rino. *The Theory of Scinillation with Applications in Remote Sensing*. Wiley, 2011.

[2] C. Rino and C. Carrano. A vector theory for forward propagation in a structured ionosphere. *Journal of Atmospheric and Terrestrial Physics*, 2021. doi.org/10.1016/j.jastp.2021.105558.

[3] C. Rino and C. Carrano. A vector theory for forward propagation in a structured ionosphere with surface reflections. *Journal of Atmospheric and Terrestrial Physics*, 2021. doi.org/10.1016/j.jastp.2021.105740.

[4] Weng Cho Chew. *Waves and Fields in Inhomogeneous Media*. A Van Nostrand Renhol, 1990.

[5] H. Bremmer. The w.k.b. approximation as the first term of a geometric-optical series. *PHilips Research Reports*, 4:189–, 1949.

[6] M. D. Feit and Jr. J. A. Fleck. Light propagation in graded index fibers. *Applied Optics*, 17:3990–3998, 1978.

[7] Louis Fishman, John J. McCoy, and Stephen C. Wales. Factorization and path integration of the helmholtz equation: Numerical algorithms. *Acoustical Society of America Journal*, 81, 1987. doi:10.1121/1.394542.

[8] Louis Fishman and John J. McCoy. Derivation and application of extended parabolic wave theories. i. the factorized helmholtz equation. *Journal of Mathematical Physics*, 25, 1984. doi.org/10.1063/1.526149.

[9] Louis Fishman and John J. McCoy. Derivation and application of extended parabolic wave theories. ii. path integral representations. *Journal of Mathematical Physics*, 25, 1984. doi.org/10.1063/1.526150.

[10] Vladimir E. Ostashev, Michael B. Muhlestein, and D. Keith Wilson. Extra-wide-angle parabolic equations in motionless and moving media. *J Acoustical Society of America*, 145(2):1031–1047, 2003. doi.org/10.1121/1.5091011.

[11] Michael D. Collins and William L. Siegmann. *Parabolic Wave Equations with Applications*. Springer, 2019.

[12] Mireille Levy. *Parabolic equation methods for electromagnetic wave paropagation*. The Institution of Electrical Engineers London, 2000.

[13] Mikhail A. Belyaev, Jeffrey Banks, and Thomas Chapman. Exact wave solver for nonparaxial laser beam propagation. *Phys. Plasmas*, 31, 2024. doi: 10.1063/5.0198523.

[14] M. Born and E. Wolf. *Principles of Optics*. Cambridge University Press, 1999.

[15] K. G. Budden. *The Propagation of Radio Waves*. Cambridge University Press, Cambridge, 1985.

[16] Christopher Coleman. Ionospheric ray tracing equations and their solution. *The Radio Science Bulletin*, 39, 2008.